Behavioural evidence for a visual and proprioceptive control of head roll in hoverflies (Episyrphus balteatus)

Roman Goulard, Alice Julien-Laferrière, Jerome Fleuriet, Jean-Louis Vercher, Stephane Viollet

© 2015. Published by The Company of Biologists Ltd | Journal of Experimental Biology (2015) 218, 3777-3787 doi:10.1242/jeb.127043

RESEARCH ARTICLE

Behavioural evidence for a visual and proprioceptive control of head roll in hoverflies (*Episyrphus balteatus*)

Roman Goulard[1], Alice Julien-Laferriere[2,3], Jérome Fleuriet[4], Jean-Louis Vercher[1] and Stéphane Viollet[1,*]

ABSTRACT

The ability of hoverflies to control their head orientation with respect to their body contributes importantly to their agility and their autonomous navigation abilities. Many tasks performed by this insect during flight, especially while hovering, involve a head stabilization reflex. This reflex, which is mediated by multisensory channels, prevents the visual processing from being disturbed by motion blur and maintains a consistent perception of the visual environment. The so-called dorsal light response (DLR) is another head control reflex, which makes insects sensitive to the brightest part of the visual field. In this study, we experimentally validate and quantify the control loop driving the head roll with respect to the horizon in hoverflies. The new approach developed here consisted of using an upside-down horizon in a body roll paradigm. In this unusual configuration, tethered flying hoverflies surprisingly no longer use purely vision-based control for head stabilization. These results shed new light on the role of neck proprioceptor organs in head and body stabilization with respect to the horizon. Based on the responses obtained with male and female hoverflies, an improved model was then developed in which the output signals delivered by the neck proprioceptor organs are combined with the visual error in the estimated position of the body roll. An internal estimation of the body roll angle with respect to the horizon might explain the extremely accurate flight performances achieved by some hovering insects.

KEY WORDS: Gaze control, Proprioception, Vision, Model, Feedback control, Dipterous, Insect, Horizon

INTRODUCTION

Gaze stabilization plays a crucial role in many tasks performed by insects during flight such as obstacle avoidance, hovering, chasing, landing and take-off. In the presence of a wide range of physical and visual perturbations, gaze is stabilized by combining cues provided by various sensory channels (Hengstenberg, 1993; Taylor and Krapp, 2007).

The main parts of this complex system, described in more detail below, are: halteres, which respond to fast body rotation; articular proprioceptive hairs, which measure joint angles; and vision, which is composed of compound eyes and ocelli. The halteres form a mechanosensory gyroscopic system that is sensitive to Coriolis forces (Nalbach, 1993; Hengstenberg, 1993, 1998; Huston and Krapp, 2009) and measure the rotational speed of the body during fast perturbations or manoeuvres and drive opposite head roll movements (Schwyn et al., 2011). An example of proprioceptive structure, the prosternal organs, consisting of a pair of mechanosensitive hair fields located symmetrically on the neck on the anterior part of the thorax of insects (Pringle, 1938; Preuss and Hengstenberg, 1992; Paulk and Gilbert, 2006), are stimulated by the head position through 'contact sclerites' (Peters, 1962). Differential stimulation of opposite sclerites during head roll movements generates mechanoreceptive cues about the head-in-body roll orientation (Preuss and Hengstenberg, 1992). Although the mechanosensory sensors located on the neck are involved in compensatory reflex responses realigning the head with the body in flies (Horn and Lang, 1978; Preuss and Hengstenberg, 1992) and are connected neuroanatomically to an insect's neck motor system (Strausfeld and Seyan, 1985; Milde et al., 1987), the exact contribution of these sensors to head control during flight has not yet been clearly established. Vision is also involved in gaze stabilization processes. It was recently established that the ocelli are able to resolve modicum spatial information (Berry et al., 2007; Hung and Ibbotson, 2014) and that the ocellar neural pathway is connected to motion-sensitive visual neurons (Parsons et al., 2006). The idea that the ocelli detect a rotation rate rather than an absolute head roll (Stange, 1981; Stange et al., 2002; Taylor, 1981a,b) has been supported by electrophysiological studies showing phasic responsiveness of ocelli to light change (Hu et al., 1978; Simmons et al., 1994; Parsons et al., 2006) and a behavioural study in which phasic head roll (~25% of compound eye maximal response) was induced by differential illumination of lateral ocelli (Schuppe and Hengstenberg, 1993), related to measurements of high-pass filter characteristics and rotational rate. The finding that head roll responses can be driven by ocellar stimulation alone has confirmed that this structure is able to operate some stabilizing reflexes (J. van Kleef, T. Massey and M. M. Maharbiz, personal communication). Moreover, on the roll axis, compound eyes are sensitive to rotational optic flow and induce compensatory head roll movements, which feature slower processing times than the ocelli (Schuppe and Hengstenberg, 1993; Hengstenberg, 1993).

Although the compound eye and the ocelli assess the rate changes in the orientation of the fly's head, they are also involved in the dorsal light response (DLR) (Mittelstaedt, 1950; Hengstenberg, 1993), which aligns the dorsal part of the head and body with the brightest part of the visual field. In the walking fly, Horn and Knapp (1984) observed the occurrence of an invariant head orientation response to the orientation of an artificial horizon despite the various body roll orientations imposed on the flies. In addition, Hengstenberg (1984) has pointed out the importance of the horizon in head roll orientation during flight and the fact that no gravity information was used to perform this task. In locusts, compensatory head roll movements were also observed in studies using an artificial horizon (Goodman, 1965; Hensler and Robert, 1990), where body roll stabilization resulted from the head stabilization that occurred in response to the DLR reaction and the changes in the horizon's

[1]Aix-Marseille Université, CNRS, ISM UMR 7287, Marseille 13009, France. [2]INRIA and Université de Lyon, Lyon 69000, France. [3]CNRS, UMR 5558, Laboratoire de Biométrie et Biologie Évolutive, Villeurbanne 69622, France. [4]Washington National Primate Research Center and Department of Ophthalmology, University of Washington, Seattle, WA 98195, USA.

*Author for correspondence (stephane.viollet@univ-amu.fr)

Received 22 June 2015; Accepted 1 October 2015

Journal of Experimental Biology (2015) 218, 3777-3787 doi:10.1242/jeb.127043

List of symbols and abbreviations

DLR	dorsal light response
$G(s)$	closed-loop transfer function of the head control
$G_h(s)$	dynamic model of the head
$H(s)$	open-loop transfer function of the head control
K	closed-loop gain
K_H	open-loop gain
Q_{head}	quantile deviation of head orientations
s	Laplace variable
S	sum of $\theta_{headbody}$ and ε_{visual}
U_{neck}	motor command
VM	visual-only model
VPM	vision and proprioception model
ε_{visual}	visual error between head and horizon orientations
$\theta_{headbody}$	angle between head and body orientations
$\hat{\theta}_{body/horizon}$	estimate of θ_{body} with respect to the horizon
θ_{body}	orientation of the body
θ_{head}	orientation of the head
$\theta_{horizon}$	orientation of the horizon
τ	closed-loop time constant
τ_H	open-loop time constant

orientation. All in all, these results suggest that visual cues predominate over gravity sense during flight, and thus support the idea that the DLR may be involved in attitude stabilization. However, although the DLR had been found to be closely linked to head and body roll steering, the interactions between gaze and the body control system still remain to be established.

Based on previous studies on the DLR, we assumed that head control in hoverflies is based solely on visual cues. The horizon is certainly a useful means of reference frame for ensuring flight stability, as we established in a first set of experiments in which the tethered flying hoverflies aligned their head with the artificial horizon presented in various orientations. These findings were supported by comparing them with the predictions of a model based on visual inputs. We then raised the question as to how the visual errors are processed when the control input signals are transmitted to both head and body. To answer this question, we perturbed the purely visual control of the head with respect to the horizon by reversing the polarity of the horizon combined with a body roll perturbation paradigm. The results obtained in this condition show that head control in hoverflies does not rely solely on a visual feedback loop and suggest that neck proprioception may act as a gateway between head and body reference frames. A new model based on both vision and neck proprioception was then drawn up in line with this assumption.

MATERIALS AND METHODS

Animals

Hoverfly pupae [*Episyrphus balteatus* (De Geer 1776)] purchased from a bio-control company (Koppert, Berkel en Rodenrijs, The Netherlands) were placed in a cage (53 cm×29 cm×29 cm) at an ambient temperature of 25±1°C until they hatched. Shortly after they hatched (less than 5 days later), males (N=8) and females (N=15) were sorted and placed in two different cages. To handle the flies and fix them on the tiny actuated clip of the roll generator, a strip of cardboard was glued (with 50% beeswax, 50% rosin) to their thorax. The state of the animals was then checked by observing their flight behaviour before returning them to the cage. They were given water *ad libitum*, surrounded by artificial flowers (carrying wet brewed pollen and sugar) and real flowers (which were replaced every 3 days). As the raising room had no windows, a photoperiod was applied artificially, using a halogen light bulb (42 W) to simulate long days lasting from 08:00 h to 21:00 h. Experiments were carried out on animals aged 3 to 21 days. The state of the animals was checked again prior to all experiments by observing their flight behaviour in the cage.

Experimental set-up

The experimental set-up used in this study was very similar to that used by Viollet and Zeil (2013) in their study on wasps. It consisted basically of a stepper motor, an opaque tube and a digital camera (see Fig. 1A). These three parts were firmly mounted onto an optical bench (Spindler and Hoyer, Gottingen, Germany) to ensure perfect alignment of the camera's optical axis with the shaft of the stepper motor (Sanyo Denki, Roissy, France; 103H5208-0440, Tokyo, Japan; 200 steps per round), which was connected to a fast electronic driver (Sanyo Denki US1D200P10). Flying animals were tethered to a tiny clamp fixed to two miniature perpendicular stages (Edmund Scientific, Lyon, France). Accurate alignment of the motor's shaft facing the camera (DALSA Genie HM640, Stemmer Imaging, Suresnes, France) was also ensured by adding two further perpendicular stages (Spindler and Hoyer) on which the motor was mounted. The motor and the camera were controlled via a data acquisition board (USB, 6128; National Instruments, Austin, TX, USA) and a fast ethernet bus connected to the camera. The stepper motor and the image acquisition set-up were synchronized with a custom-written LabVIEW-based program (National Instruments, Austin, TX, USA) running on a PC. Movie sequences were stored frame by frame in the form of uncompressed 8-bit tiff images (resolution: 640×480 pixels) for off-line processing. Special attention was paid to the choice of ethernet board (Intel Pro/1000 GT Desktop Adapter) to ensure a maximum rate of 200 frames s^{-1} without any loss of images during the experiments. Each experiment lasted 20 s. Hoverflies were placed inside an opaque tube (internal diameter, 9.5 cm; length, 20 cm) illuminated frontally by an fibre optic ring light (Schott, KL 1500, Clichy, France; 8.32×10^{-9} W m^2) fitted with a halogen light source (Xenophot HLX, OSRAM, Molsheim, France) and three pairs of infrared LEDs were used to light the hoverfly when the ring light was turned off. The digital camera was used to film the head and body movements (see Fig. 1C). After introducing a hoverfly into the tube, it was presented with various patterns: a tilted artificial horizon (a half-black, half-white roll of paper presented in various orientations, as shown in Fig. 1B) and a uniform white background. A gentle air stream generated by a compressor (Silent Air System SAS-038, Oil-free, Dürr Technik, Bietigheim-Bissingen, Germany) connected to a small flexible tube (diameter, 6 mm) was directed towards the fly during all the experiments in order to induce and sustain flight behaviour.

A purely vision-based model

In light of previous studies showing that visual systems (including compound eyes and ocelli) are involved in the gaze stabilization reflex, the DLR was *a priori* modelled in the form of a single visual feedback loop, which is presented in detail in Fig. 2. The visual error (ε_{visual}) results here from the difference between the horizon orientation ($\theta_{horizon}$) and that of the head (θ_{head}). At each time-step, the 'head in body' orientation ($\theta_{headbody}$) is adjusted in response to the horizon's orientation based on the visual error. Then, by definition, the output of the system θ_{head} was obtained by adding $\theta_{headbody}$ with θ_{body}. Behavioural experiments will allow us to validate this model.

Static condition

The angular position of the motor's shaft was adjusted to keep the hoverfly's body horizontal. Once a hoverfly had been placed in the tube and the light turned on, it was surrounded by an artificial horizon oriented in any of five different directions: −90 deg, −45 deg, 0 deg, 45 deg and 90 deg (negative angles with clockwise tilts and positive ones with counterclockwise ones; see Fig. 1B). The head response was also measured in the absence of any orientation cues (with a uniform white background). At the end of each run, the fly was removed from the tube, the orientation of the pattern was changed and after a short rest, further runs were conducted until all five orientations and the uniform background had been experienced by the insect. The same hoverfly could not undergo more than one set of runs per day, and if any of them showed a complete lack of flight motivation, the experiment was stopped and possibly resumed later in the day. Flight behaviour was induced and maintained by a gentle frontal air flow.

Journal of Experimental Biology

Journal of Experimental Biology (2015) 218, 3777-3787 doi:10.1242/jeb.127043

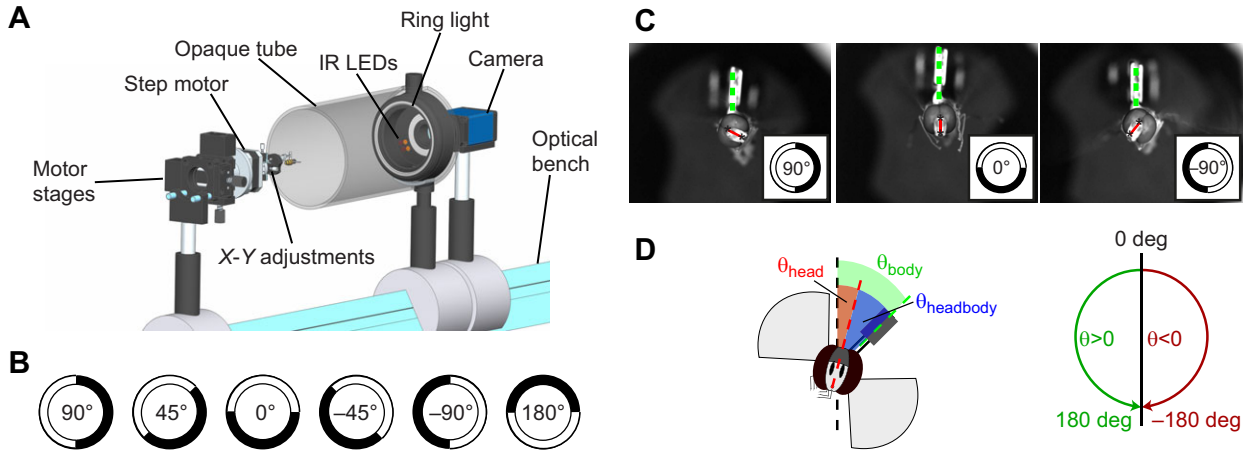

Fig. 1. Experimental set-up. (A) Hoverflies were tethered by attaching a strip of waxed cardboard to their thorax and mounted onto the shaft of a step motor. Flies were presented with various patterns while being filmed head-on with a digital camera at a rate of 200 frames s^{-1}. (B) An artificial horizon, consisting of a half white, half black printed paper roll, was presented to the hoverfly in six different orientations ranging from –90 deg to 90 deg, including an upside down horizon (180 deg). Patterns were held in place by an opaque cylinder and illuminated with a fibreoptic ring light placed in front of the insect and three pairs of infrared LEDs (to record the insects' movements during experiments performed in complete darkness, see Materials and methods). (C) Sample images of hoverflies under static conditions with three different orientations of the artificial horizon. Cyan asterisks indicate the natural markers which were used to determine the head orientation (red dashed line). The orientation of the body, which is given by the green dotted line, was taken here to be equal to 0 deg. (D) During the static experiments, only the head orientation (θ_{head}) was measured and the body orientation (θ_{body}) was assumed to be null, whereas θ_{body} was also determined during step responses by measuring the orientation of the cardboard placed in the clamp. Orientation of the head with respect to the body ($\theta_{headbody}$) was calculated by applying: $\theta_{headbody}=\theta_{head}-\theta_{body}$. Angles were taken to be positive in the counter-clockwise direction from the head-on viewpoint, and negative in the clockwise direction, with regards both the fly's position and that of the artificial horizon.

Light off/on condition

To identify the dynamic of the control underlying head locking to an artificial horizon we measured the response to a step. The motor's shaft was adjusted to keep the fly's body horizontal. Once a hoverfly had been introduced into the tube lined with an artificial horizon oriented in one of the four different positions (−90 deg, −45 deg, 45 deg and 90 deg) with the light turned off, the light was switched alternately on and off approximately every 5 s manually during the run, giving two dark sequences followed by two illuminated sequences per 20 s run. Flight was filmed during the dark phases under infrared LED lighting in front of the animal. The flies were removed from the tube at the end of the run and the horizon's orientation was changed until the insect had been exposed to all four orientations. Flight behaviour was induced and maintained by a gentle air flow from the front.

From these behavioural data, a transfer function was identified and used to model the visual processing and control dynamics. Neck muscle dynamics and head inertia were represented by another transfer function with a 5 ms time constant compatible with low inertia and mass of the head and quick neck actuation (Viollet and Zeil, 2013). Because this time constant corresponds to our recording sample frequency, we assume that

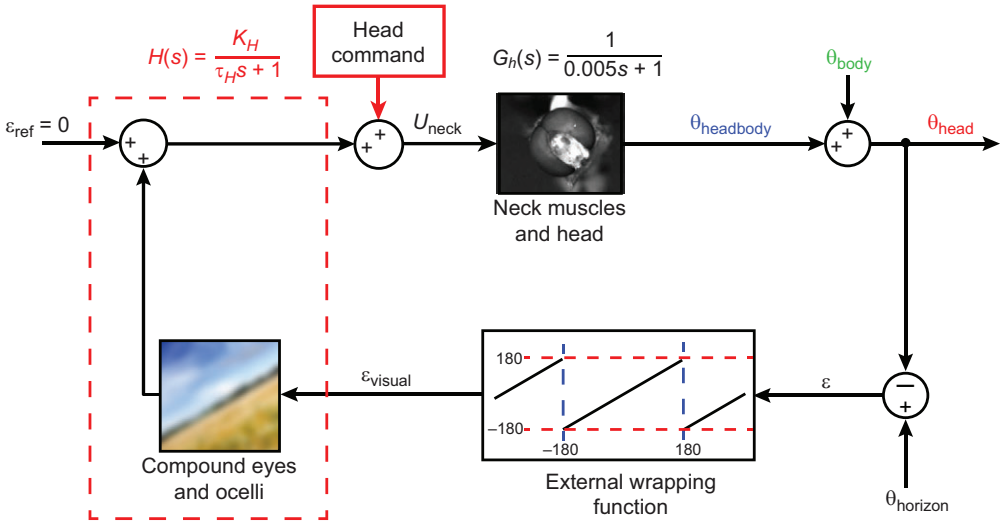

Fig. 2. Block diagram of the vision-based closed-loop control used to describe the insects' responses to an artificial horizon. The input to the system is the orientation of the horizon ($\theta_{horizon}$); the error ε is the difference between $\theta_{horizon}$ and θ_{head}; ε_{visual} corresponds to the retinal projection of the horizon (ranging from [–180 deg to +180 deg]); ε_{visual} is then used as the control input signal to the neck muscles U_{neck}, making the head rotate with respect to the body ($\theta_{headbody}$). Lastly, $\theta_{headbody}$ and θ_{body} are summed, yielding by definition the output signal θ_{head}. A first-order transfer function ($H(s)$) represents the visual processing and control dynamic, neck muscles dynamics and head inertia are modelled also by a first-order transfer function noted $G_h(s)$ with a 5 ms time constant compatible with low inertia and mass of the head and quick neck actuation.

Journal of Experimental Biology

Journal of Experimental Biology (2015) 218, 3777-3787 doi:10.1242/jeb.127043

identified transfer functions only correspond to control dynamic and not to actuator one. In practical terms, the toolbox identification provided with MATLAB was used to extract the closed-loop transfer function corresponding to the output/input [noted $G(s)$] from light off/on experiments. Then the open-loop transfer function $H(s)$ was calculated according to the Mason rules (Franklin et al., 1994):

$$\begin{cases} G(s) = \theta_{head}/\theta_{horizon} = \dfrac{K}{\tau s + 1} = \dfrac{H(s)}{1 + H(s)} \\ H(s) = \dfrac{K_H}{\tau_H s + 1} = \dfrac{G(s)}{1 - G(s)} = \left(\dfrac{K}{1-K}\right) / \left(\dfrac{\tau s}{1-K} + 1\right) \end{cases}, \quad (1)$$

whence it appears that:

$$\begin{cases} K_H = \dfrac{K}{1-K} \\ \tau_H = \dfrac{\tau}{1-K} \end{cases}, \quad (2)$$

with K and τ the identified parameters of the closed-loop transfer function $G(s)$ and s is the Laplace variable. Simulations were made with MATLAB-Simulink, with a time-step of 0.005 s, to confirm the identification (see blue line in Fig. 6). Only roll around the animal's longitudinal axis was considered, allowing us to describe a single input–single output (SISO) system. The model was restricted to the effects of a static horizon, and the responses elicited via motion-sensitive and mechanosensory channels (modelled in Schwyn et al., 2011) were not taken into account.

Body rotation with an upside-down horizon

To test the model to its limits we put hoverflies in an uncommon visual environment. The artificial horizon was settled in an upside-down configuration (black on top and white on bottom of the visual field, 180 deg of the 0 deg horizon). The step motor's shaft was rotated to orient the hoverfly's body at an angle of approximately 30 deg in the initial state. A series of brisk angular steps rotating the fly's body by ±60 deg within 0.05 s (rotational speed of 1200 deg s^{-1}) was applied every 5 s (0.2 Hz). Flight behaviour was induced and maintained by a gentle frontal air flow.

Images analysis

Head orientation (θ_{head}) was obtained during the body rotation experiments by tracking two natural markers on the fly's head (Fig. 1C) with a semi-automatic marker-tracking software program running under MATLAB (Hedrick, 2008). Body orientation (θ_{body}) was taken to be 0 deg under static and light off/light on conditions and measured via the orientation of the cardboard during rotation, which was determined automatically with another custom-made MATLAB program. The $\theta_{headbody}$ angle was calculated in the form of the difference between θ_{head} and θ_{body}.

Two variables were used to analyse the results of the static experiments. The first was the mean head orientation (denoted $\overline{\theta_{head}}$). One value of $\overline{\theta_{head}}$ was extracted from each run analysed.

The second variable was the quantile deviation between 10th and 90th [denoted Q_{head}, Zar (1996)] in all the orientations observed during a run (at 200 frames s^{-1}), as given by the following equations:

$$Q_{head} = \frac{90^{th}_{centile} - 10^{th}_{centile}}{2} \quad (3)$$

where Q_{head} is half the difference between the maximum and minimum values of 80% of θ_{head} data, in view of the fact that 10% were excluded on both sides of the data distribution (2×2 s at most) in order to prevent occasional artefacts from increasing the value of Q_{head}. Therefore Q_{head} was our proxy for θ_{head} stability during each run: the more the θ_{head} values were

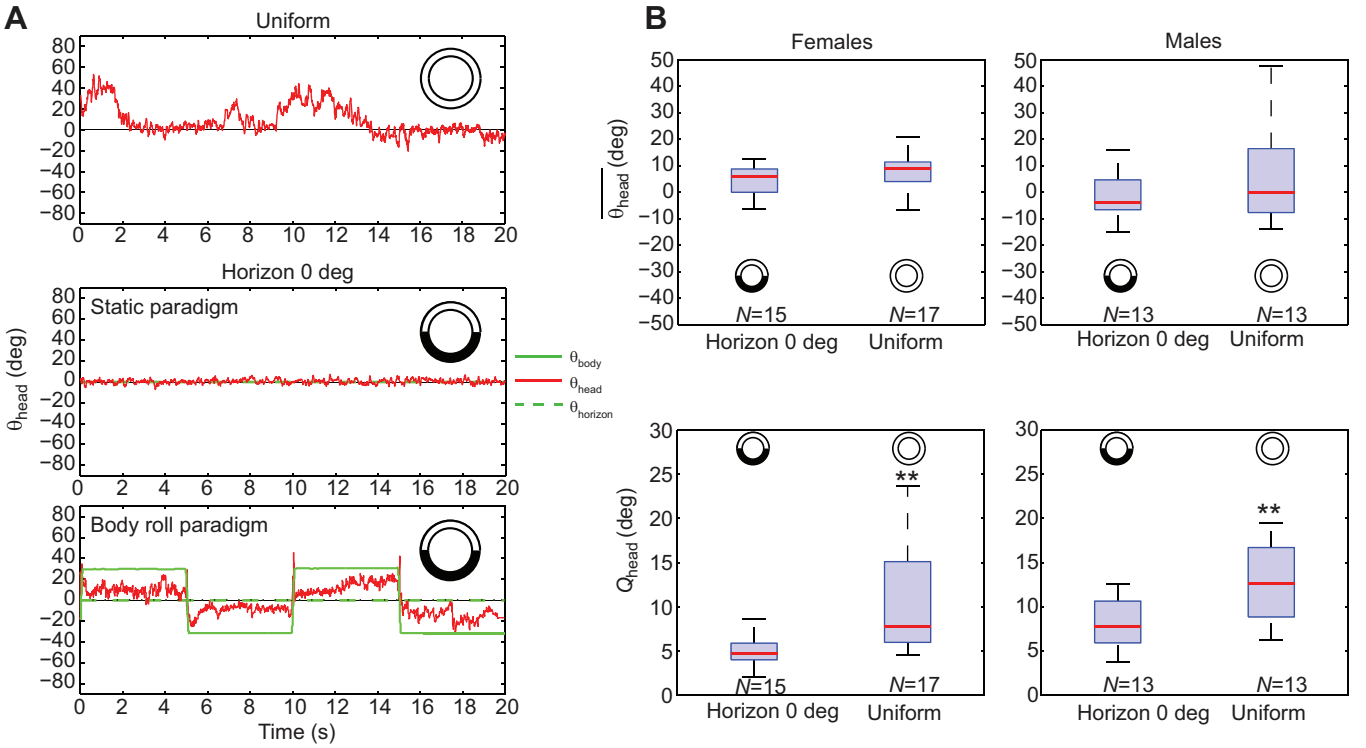

Fig. 3. Uniform versus artificial horizon head responses. (A) Example of time courses of θ_{head} recorded with a horizon and a uniform background in static condition (top and middle panels). Head responses showed small saccades and drift without any visual cues in uniform surroundings, whereas the head remained still in space in the presence of the artificial horizon. Bottom panel is an example of the body roll paradigm with a 0 deg horizon. Hoverflies tend to correct misalignment with horizon induced by body movement; nevertheless, a steady-state error persists. (B) Boxplots showing female and male mean head orientation (top panels, $\overline{\theta_{head}}$) and quantile deviation (bottom panels, Q_{head}) between 10th and 90th centile of the head orientation during 20 s trials with a uniform background and the artificial horizon in static condition. The number of runs N is given in each boxplot. The LME model procedure (see Materials and methods) showed the existence of a slight effect of no horizon cues on $\overline{\theta_{head}}$ (P=0.08, F=3.08) and a significant effect on Q_{head} (**P<0.01, F=11.73).

Journal of Experimental Biology (2015) 218, 3777-3787 doi:10.1242/jeb.127043

scattered during a run, the higher the Q_{head} value tended to be and the lower the stability of the head was. One value of Q_{head} was extracted from each run.

Statistical analysis

Linear mixed-effects (LME) models were used to discriminate between the effects of the artificial horizon, its orientation ($\theta_{horizon}$) and the sex of individuals (fixed effects) on both $\overline{\theta_{head}}$ and Q_{head}. As each individual was liable to undergo several trials, the date of the experiments was also included as a fixed effect in order to rule out the potential effects of habituation processes, and individuals were included as a random effect. The Akaike information criterion (AIC) was used to compare and select the best LME model and an ANOVA analysis was then applied to this model to determine the significance (the *P*-value) of the effects. All the statistical analyses were conducted with freeware R software (www.r-project.org).

RESULTS

Head roll stabilization in the presence of an artificial horizon

Typical time courses of θ_{head} during tethered flight with an artificial horizon or a uniform background are shown in Fig. 3A. The uniform background condition induced visible drifts in the head orientation, whereas no drifts were observed in the presence of the artificial horizon and the head remained very still in space. In both conditions, we observed small-amplitude head saccades, around 5 deg for the artificial horizon and 10 to 20 deg for the uniform background.

As shown in Fig. 3B, in the presence of the artificial horizon, the range of hoverflies' head orientations decreased significantly (bottom panels) during tethered flight ($P<0.01$). Their mean head orientations also shifted slightly counter-clockwise (top panels) during flight by a median value of less than 5 deg (shift was not significant, $P=0.08$) between the uniform pattern and the trials with an artificial horizon in the case of both males and females. As shown in the boxplots, the inter-run variability of $\overline{\theta_{head}}$ increased with the uniform background, especially in the case of males.

Influence of a tilted horizon

Fig. 4 shows one typical time-course corresponding to each orientation of the horizon (see Fig. 1B) except for the horizontal orientation (0 deg, see Fig. 3). As expected from previous experiments (Hengstenberg, 1984; Hensler and Robert, 1990; Goodman, 1965), horizon orientations ranging from −90 deg to +90 deg gave rise to a clear-cut change in the insects' head orientation, the direction of rotation of which was that imposed by the horizon's inclination. The hoverfly was unexpectedly able to episodically orient its head and keep its orientation almost entirely locked to the horizon when the latter was rotated by ±90 deg. As shown in Fig. 4B,D, no responses to the orientation of the horizon were produced during non-flying periods, as reported by Hengstenberg et al. (1986) and these phases were therefore excluded from our analysis. Fig. 4A,C shows that the flies' responses were often incomplete and included a non-null steady-state orientation error between the head and horizon.

In Fig. 5A,B, similar significant correlations ($P<0.001$) were obtained with males or females between the orientation of the artificial horizon and the mean orientation of the head recorded during a run. Fig. 5C,D shows the existence of a significant difference in the dispersion of θ_{head} during a run between sexes: females showed greater head roll stability than males. However, regardless of sex, the head orientation recorded with a 0 deg artificial horizon was also significantly more stable than with any other orientation of the horizon ($P<0.001$). The inclination of the head frequently showed the occurrence of a steady-state error in response to the inclination of the horizon, despite large rotations of the artificial horizon up to ±90 deg. The median value of $\overline{\theta_{head}}$ ranged between ±25 deg, nevertheless, several males (≈25%) were able to keep their head rotated in average larger than +50 deg during 20 s runs when the artificial horizon was inclined by +90 deg. The

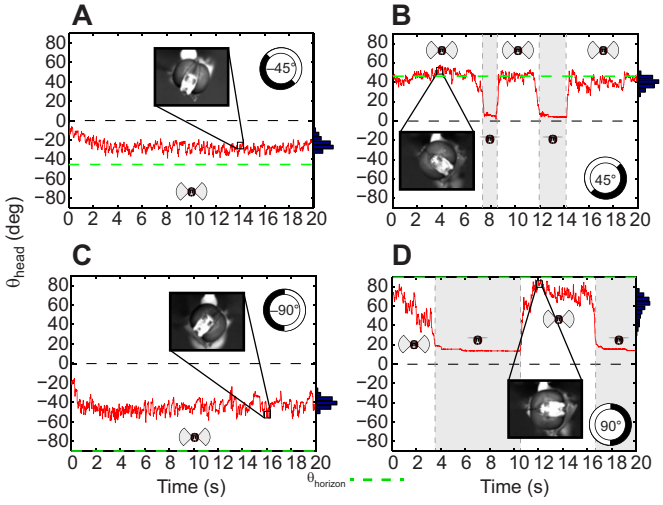

Fig. 4. Examples of head roll versus various horizon orientations. Examples of time courses of θ_{head} during one run with various orientations of the artificial horizon for a female (A,C) and a male (B,D). Photos in the insets give an example of the head roll in each condition. When the horizon was rotated by 90 deg, several males were unexpectedly able to keep their heads rotated by about 80 deg. On the right side of each figure, the probability density function of θ_{head} is plotted during a 20 s run. As shown in B and D (45 deg and 90 deg), only the temporal sequences corresponding to active flight were included in the analysis and the probability density function calculations, whereas non-flying period was omitted (grey shaded area).

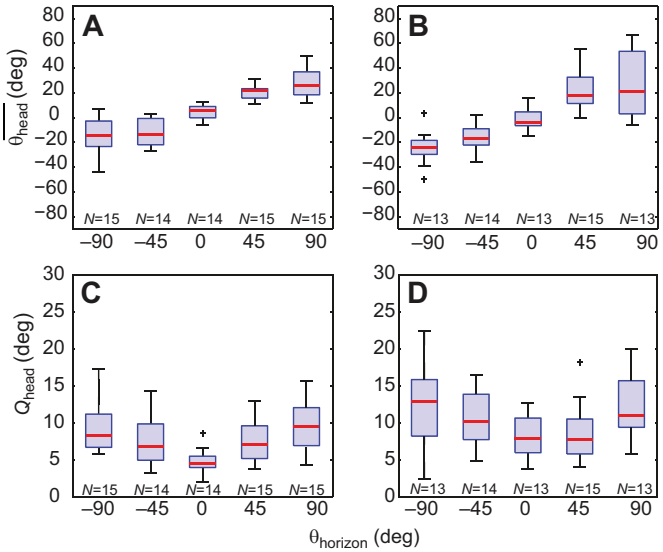

Fig. 5. Steady-state response of the head roll to various horizon orientations. Boxplots of mean head orientation (A,B; $\overline{\theta_{head}}$) and quantile deviation (C,D; Q_{head}) between 10th and 90th centile of head orientation during 20 s trials in the five different orientations of the artificial horizon (the number of runs *N* is given on each boxplot) in female (A,C) and male (B,D) flies. The LME procedure selected a significant effect of the artificial horizon orientation on $\overline{\theta_{head}}$ (***$P<0.001$, $F=245.208$) and a significant effect of sex on Q_{head} (**$P<0.01$, $F=9.057$). A supplementary ANOVA showed the presence of a significant effect between 0 deg artificial horizon and other horizon orientations on Q_{head} (***$P<0.001$, $F=11.74$).

Journal of Experimental Biology

Journal of Experimental Biology (2015) 218, 3777-3787 doi:10.1242/jeb.127043

correlations between the mean head response and the orientation of the horizon were consistent with the vision-based model (VM, see Fig. 2). However, since the correlation between $\overline{\theta_{head}}$ and $\theta_{horizon}$ was found to be lower than 1, the insects' responses may have been constrained here by a saturation mechanism: this point will be discussed below.

Dynamics of head locking to an artificial horizon

To study the temporal dynamics of head roll versus various orientations of the horizon, the hoverfly was placed in complete darkness and the light was suddenly turned on in the cylinder. Fig. 6 gives the average response of hoverflies to the sudden onset of the light, enabling the fly to detect the presence of an inclined artificial horizon. Once the light had been switched on, the head rotated directly in the direction imposed by the inclination of the artificial horizon. The step response of the head roll closely matched the step response of a first-order system described by the visual feedback loop model. We identified the output/input relationship, i.e. $\theta_{head}/\theta_{horizon}$. Because the neck and head inertia time constant is in the same order as the recording frame rate (0.005 Hz), we neglected them during the identification process. The control transfer function $H_{(s)}$ was calculated as follows (see Materials and methods, light off/on experiments):

$$\begin{cases} K_H = \dfrac{K}{1-K} \\ \tau_H = \dfrac{\tau}{1-K} \end{cases}. \quad (4)$$

Table 1 shows the great variability of the gain K, which determined the final value of the step response. As expected for a dynamic in a system with no integrator, the higher K was, the less the steady-state error became. In control engineering, at least one integrator is necessary in a closed-loop model to be able to reach a null steady-state error in response to a step. Although the previous finding that locusts' responses featured a zero steady-state error under free-roll conditions (Goodman, 1965) suggested the existence of an integrator, the step responses measured in our tests featured steady-state errors. In view of these findings, no integrator was included in the model, although these errors may be attributable to the tethered condition, which may have induced proprioceptive conflicts (see the Discussion). In addition, males showed higher K than females under all the orientation conditions tested, whereas the term τ, which is the time constant of the response, seems to have been very consistent in females, where it ranged between 0.1 s and 0.2 s. The time constant was again larger in males than females and varied between approximately 0.3 s in the case of negative (clockwise) rolls and 1 s in that of positive (counter-clockwise) ones. This unexpected difference between clockwise and counter-clockwise response dynamics is unexpected and difficult to explain, but it may have been due to uncontrollable airflow heterogeneity in the tube exerting differential forces on the neck. It is worth noting that the head roll induced by the artificial horizon never involved head saccades but always involved a smooth head rotation.

Head responses with an upside-down horizon

A reversed artificial horizon (with an orientation of 180 deg) was used here in order to saturate the control input signal sent to neck muscles. In these experiments, periodic (0.2 Hz), 60 deg amplitude steps were applied to the body, consisting of a transient 0.05 s phase (1200 deg s^{-1}) and a 4.95 s static phase. The insect's body was initially tilted by an angle of +30 deg in order to avoid having a perfect 180 deg alignment between horizon and head (which could have led to ambiguities) and this made it possible to establish that the head roll occurred in the direction that minimized the difference between the orientation of the head and that of the horizon. We only included in the analyses sequences in which the flies showed head roll amplitudes greater than ±60 deg before the onset of a body perturbation (50% and 27% of males and female sequences, respectively). Fig. 7B shows that hoverflies tried to correct the error between their head and the upside-down artificial horizon.

In the initial closed-loop model presented in Fig. 2, we simply included a measurement of θ_{head} relative to $\theta_{horizon}$ as a visual output controlling the head. Based on this simple model, the simulated response of the VM model shows that when the horizon is in the upside-down configuration, an angular step applied to the body will modify only the amplitude of the head roll, not its sign (Fig. 7B, red

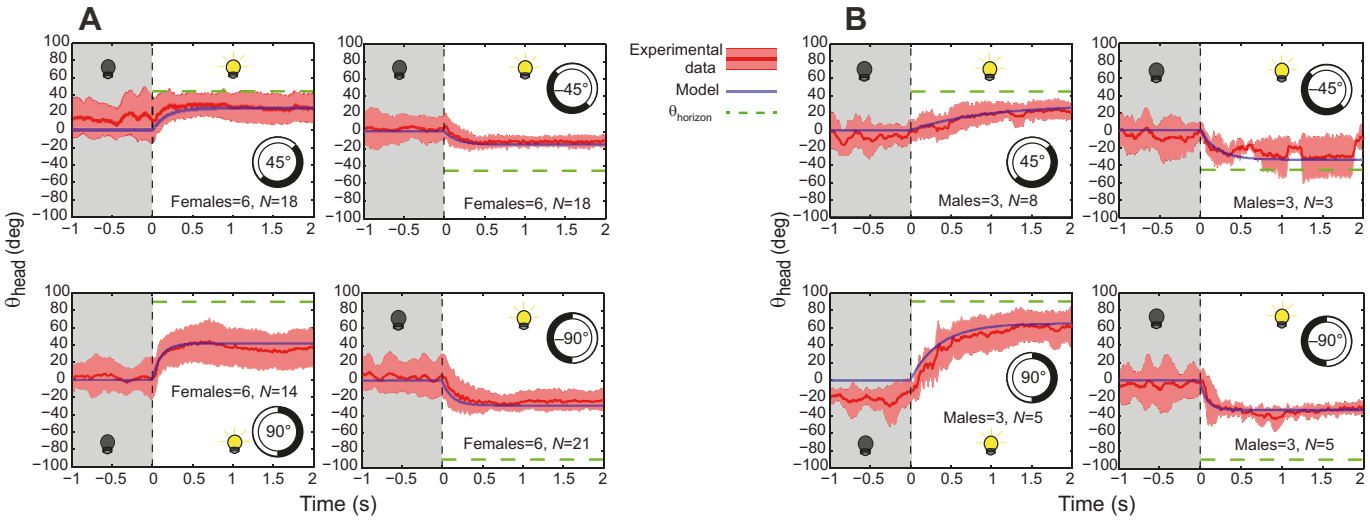

Fig. 6. Head roll dynamics during transitions from darkness to light. Mean female (A) and male (B) head roll responses (solid red line; ±s.d., coloured envelope) to a sudden onset of the lighting enabling the fly to detect the presence of an inclined artificial horizon with four different orientations (green dashed lines). Only the period starting 1 s before (grey shaded zone) and ending 2 s after the light turned on was taken into account. Head roll responses were modelled using a first-order transfer function (blue line), the mean parameters used are summarized in Table 1. Number of hoverflies and number of trials N in each orientation are specified.

Journal of Experimental Biology (2015) 218, 3777-3787 doi:10.1242/jeb.127043

Table 1. Output/input function identification from light off-on experiments described in Fig. 6

	$\theta_{horizon}$	Females		Males	
		K	τ(s)	K	τ(s)
$G(s)$	45 deg	0.55±0.33	0.16±0.10	0.65±0.10	0.92±0.60
	−45 deg	0.35±0.15	0.10±0.08	0.76±0.43	0.21±0.16
	90 deg	0.46±0.27	0.11±0.08	0.72±0.15	0.36±0.10
	−90 deg	0.32±0.12	0.12±0.10	0.38±0.07	0.09±0.06
$\hat{\tau}$	–		0.12		0.39

Parameters of the closed-loop transfer function, output/input function, describing head roll step responses for each orientation of the artificial horizon ($\theta_{horizon}$). A transfer function was estimated for each averaged individual response for each horizon orientation and K and τ parameters are presented along with±the inter-individual s.d. LME statistical model reveal a significant effect of the sex of individuals on τ (**P<0.01, F=10.99), a significant effect of the orientation of the horizon on the gain K (*P<0.05, F=4.91) and a slight effect of sex on the gain (P=0.06, F=4.73). $\hat{\tau}$ has been averaged from all orientation for females and males as statistical analysis did not show a significant effect of the orientation on τ values (P=0.12, F=3.04 for males and P=0.91, F=0.01 for females) to be used in model simulations.

dashed lines). However, contrary to the VM model response, hoverflies quickly rotated their head in the same direction as that imposed by their body roll in the steady state (see Fig. 7B, red lines).

DISCUSSION

This study focused on the reaction of a visuomotor reflex in charge of controlling the head orientation with respect to the horizon in hoverflies. In this section, a new model for the visuomotor reflex is presented and the possible role of the neck proprioceptor organs combined with visual information is discussed.

Gaze locking to the horizon

The results obtained here show the importance of head locking to an artificial horizon in hoverflies. In particular, they show that the key feature of this response was the white/black polarity of the horizon rather than the contrast edge (Hengstenberg, 1984). The presence of an artificial horizon during flight enables the flies to control their angular head position more accurately. This is a complementary way of adjusting the head's angular speed to that based on optic flow measurements, which has been described as a head roll stabilization process in wasps (Viollet and Zeil, 2013). In addition, stabilizing the head with respect to the horizon greatly simplifies the visual processing by providing a steady reference frame (Taylor and Krapp, 2007). In his studies on blowflies, Hengstenberg (1984) observed that starting at wingbeat initiation, flies took several seconds to turn their heads toward a previously tilted horizon. Contrary to these findings, we did not observe any delay in the hoverflies' responses during the phases when they stopped and started flying again (see Fig. 4). With a horizon tilted by ±90 deg, only a few males were able to turn their head more than 50 deg. One possible explanation for this finding might be the existence of a mismatch between the sensorimotor feedback loops and the insects' visually guided behavioural command under tethered conditions (Zeil et al., 2008). This explanation is coherent with the fully compensatory responses recorded in locusts under free body roll conditions, where the head and body could be perfectly aligned with a light source (Goodman, 1965). However, we consistently observed here that the head of the flying hoverflies compensated for tilted horizons and the extent of their responses to the upside-down configuration certainly shows the importance of the horizon as a zero reference for head control. This finding rules out the hypothesis that these responses may be based purely on local edge detection mechanism, as observed in previous studies (Hengstenberg, 1984), or on differences in lighting between the two sides (Neumann and Bülthoff, 2001), regardless of the contrast. By contrast, the head responses measured here, especially those obtained with the upside-down horizon and the ±90 deg tilted horizon, show indeed that the polarity of the horizon contributes to these responses. The large head rolls measured in the presence of the reversed horizon suggested that a large-field integration has been mediated by the compound eye rather than the ocelli, which have rather narrow visual fields (Schuppe and Hengstenberg, 1993). The

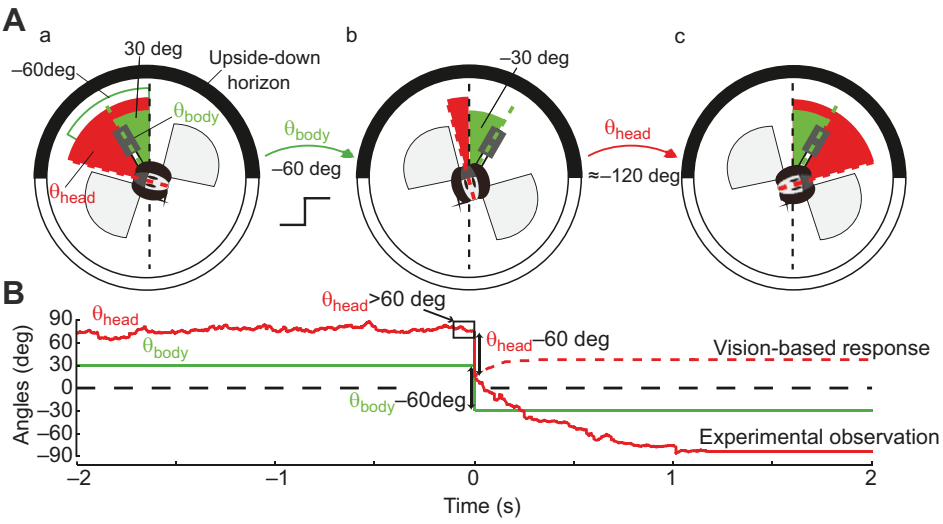

Fig. 7. Reversed head roll behaviour with an upside-down horizon during body steps. (A) Sequential diagram of the head roll control observed (a) when the hoverfly was initially surrounded by the reversed horizon and its body was initially rotated by +30 deg. Head roll was directed in the direction minimizing the difference between its orientation and that of the horizon. (b) The fly was then subjected to a clockwise angular step of 60 deg applied to its body. (c) Instead of compensating for the horizon as predicted by the visual feedback loop model, the head rotated by approximately −120 deg so that it was oriented in the same direction as that imposed by the body roll in the steady state. (B) Time course of the head and body roll according to the sequential diagram presented in A for behavioural data and vision-based model.

Journal of Experimental Biology (2015) 218, 3777-3787 doi:10.1242/jeb.127043

ocelli have been found to drive some compensatory head reflexes (J. van Kleef, T. Massey and M. M. Maharbiz, personal communication) and seem to play a role in the initiation of DLR, decreasing the response latency (Stange, 1981; Taylor, 1981a; Parsons et al., 2006). It has been established that the ocelli are characterized by faster visual processing than the compound eye (Hengstenberg, 1993; Taylor and Krapp, 2007) and motion direction sensitivity (Berry et al., 2007; Hung and Ibbotson, 2014). In dragonflies, fast alternating optical stimulation of the lateral ocelli triggered strong compensatory head roll movements (Stange, 1981). The procedure used in the latter study also showed the occurrence of phasic responses to light changes triggered by ocellar inputs. To summarize, the reversed horizon paradigm might be a useful means of elucidating the respective contributions of the ocelli and the compound eyes.

Model based on vision and proprioception (VPM)

The second aim of our study was to look more closely at the coupling existing between head control and body control. For this purpose, we set the system to its limits and compared the results obtained with the responses of the VM model. In the presence of an upside-down horizon and body perturbations, the purely visual feedback loop did not account satisfactorily for the compensatory head roll process. With regard to limits of the VM model, we tried to enhance it by adding proprioceptive information. First, because halteres had only been linked so far to compensation against body perturbation and therefore could not explain head reversal observed (see Fig. 7), we only focused on the role of neck joint proprioception. We therefore added the 'head in body' orientation provided by neck proprioceptors, among which prosternal organs have been previously studied and found to be involved in neck motor responses (Liske, 1977; Preuss and Hengstenberg, 1992; Paulk and Gilbert, 2006). The existence of multisensory contributions to gaze stabilization is not surprising in view of the many channels involved (Hengstenberg, 1993; Taylor and Krapp, 2007). In insects, multimodal sensory convergence was found by electrophysiological studies between the halteres and vision in flies (Huston and Krapp, 2009) or between proprioceptive and visual motion-sensitive neurons known as 'self-movement detectors', which are involved in the flight control feedback system in dragonflies (Olberg, 1981). Such an integration pattern is supported by neuro-anatomical convergence occurring around the neck motor neurons in flies (Strausfeld and Seyan, 1985; Milde et al., 1987). It follows that the responses shown in Fig. 7 suggest that the fly may be endowed with a sensorimotor system that prevents its head from reaching undesirably large roll angles. Consequently, we enhanced the system (see Fig. 8) by summing neck proprioceptor organ input ($\theta_{headbody}$) and visual error (ε_{visual}) and kept the result S in geometrical constraint of [−180 deg, 180 deg], with an internal wrapping function. We showed that an estimation of the orientation of the body in horizon could be obtained by adding visual and proprioceptive inputs:

$$\begin{aligned} S &= \varepsilon_{visual} + \theta_{headbody} \\ &= \theta_{horizon} - \theta_{head} + \theta_{head} - \theta_{body} \\ &= \theta_{horizon} - \theta_{body}. \end{aligned} \quad (5)$$

Simulations were conducted directly by using the first-order transfer function with mean time constant $\hat{\tau}$ for males and females averaged from the closed-loop identification presented in Table 1, whereas the gain K was adjusted in line with the head dynamics. This new VPM model based on visual and proprioceptive information responds in line with behavioural observations to sudden change of body attitude in the upside-down horizon configuration (see Fig. 9).

An objection to our model could be that it is only useful, in comparison with the VM model, under specific conditions where

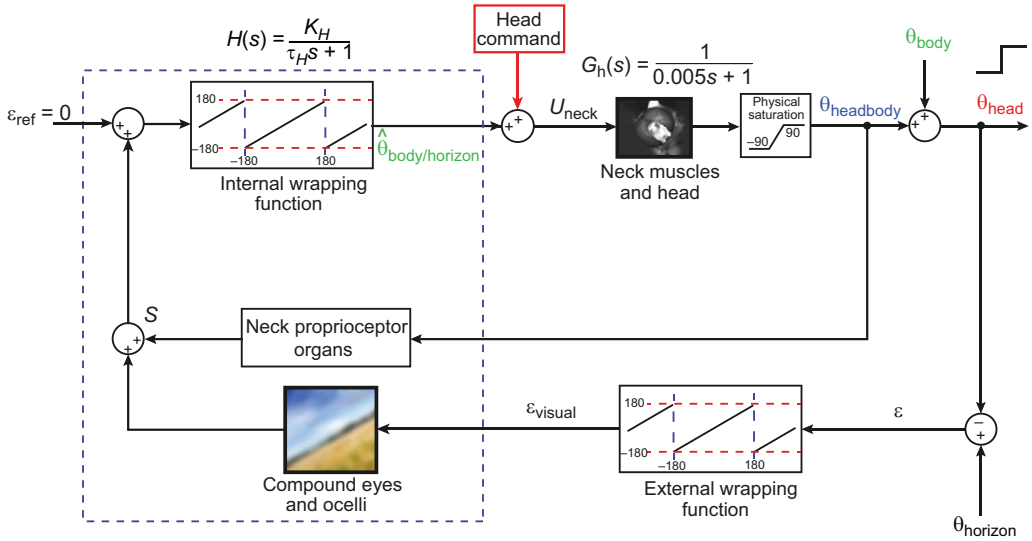

Fig. 8. Block diagram of the enhanced model for head locking to the horizon. The visual measurement (ε_{visual}) of the horizon's orientation is based here on the difference (ε) between the horizon's orientation and that of the head. A wrapping function keeps the visual error (ε_{visual}) in the [−180; 180] range. The visually induced error of the head orientation with respect to the horizon is therefore now summed together (S) with the neck proprioceptor output signal corresponding to the 'head in body' orientation. We assumed that this sum stays in the [−180; 180] range based on the internal wrapping function possibly implemented in the fly, where S is equal to the orientation of the body with respect to the horizon ($\hat{\theta}_{body/horizon}$). This sum is directly used in the model as the neck motor command (U_{neck}). The first-order transfer function [$H(s)$] includes the visual processing and the controller dynamics, whereas the neck muscle dynamics and head inertia are also modelled using a first-order transfer function [$G_h(s)$] with a 5 ms time constant, which is compatible with low head inertia and quick neck actuation. A supplementary head command box had been added to the model in order to simulate an arbitrary control input signal originating from another pathway, which does not interfere with the two nested feedback loops (see Fig. 10).

Journal of Experimental Biology

Journal of Experimental Biology (2015) 218, 3777-3787 doi:10.1242/jeb.127043

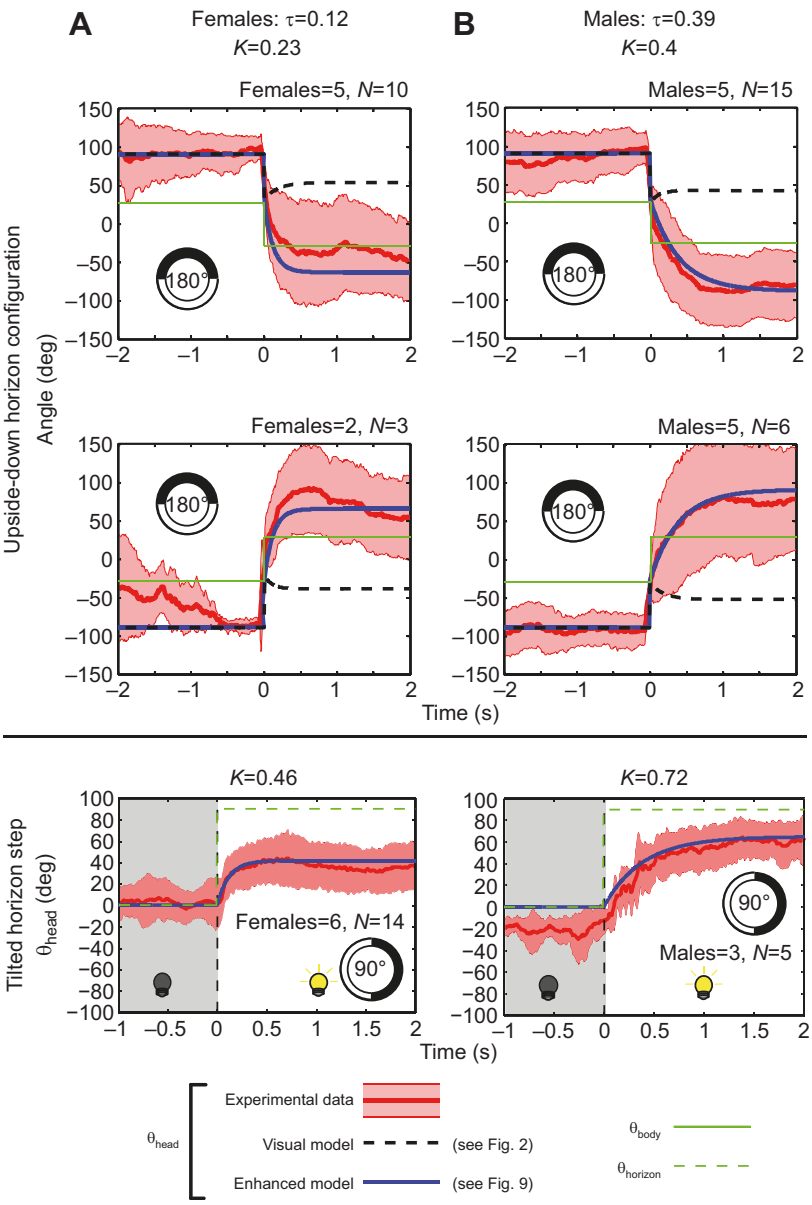

Fig. 9. Head roll with a reversed horizon. Experimental responses (red line, average response; coloured envelope, s.d.) for (A) females and (B) males plotted along with the simulated visual model responses (dashed black line) and the enhanced model (blue line) during the ±60 deg body steps (green line) with an upside-down artificial horizon (tilted by 180 deg; top panels in A,B) and during a simulated step of horizon tilt from 0 deg to 90 deg compared with light off/on experimental data (bottom panels in A,B). The gain *K* was adjusted independently for upside-down horizon because of the physical saturation of the neck whereas for 90 deg tilt, *K* was equal to open-loop transfer function identification. τ values were based on the sex-averaged time constant given in Table 1.

the animal is in an upside-down position, which does not occur very frequently under natural conditions. In any case, the performances of the new model are similar to the VM model's step responses (see Fig. 9). Unlike the VM model, however, the enhanced model presented in Fig. 8 not only accounts for the head roll measured in response to various orientations of the horizon, but also sheds new light on the hoverfly's ability to estimate its own body orientation relative to the horizon ($\widehat{\theta}_{body/horizon}$) using neck-proprioceptor organs (Eqn 5).

Although we have described and modelled the gaze stabilization process with respect to the horizon in hoverflies, it still remains to be determined how visual information contributes to controlling the body's attitude. Previous studies have focused on the linear relationships between head and body control input signals during yaw rotations, body movements copying head movements in the controversial delayed responses observed by Land (1973) and the simultaneous responses observed in flies (Geiger and Poggio, 1977), bees (Boeddeker et al., 2010) and wasps (Viollet and Zeil, 2013). Even on the roll axis, Goodman (1965) attributed the inability of locusts to realign their head and body without having any prothoracic hair and hair plate to the disappearance of the neck realignment reflex. Yaw and roll gaze-stabilization strategies are known to differ (Schilstra and van Hateren, 1998). Since the roll attitude control system is directly involved in fly stability (Hengstenberg, 1984), it seems unlikely that a strategy based only on an automatic realignment of the body with respect to the head will suffice to stabilize the body during roll movements. As observed by Collett and Land (1975), translational flight in hoverflies requires a tilted orientation of the thorax, while the head remains horizontal. The predictions of the present model suggest that the estimated body roll might be compared with a reference input signal allowing the fly to initiate an arbitrary body roll movement. On similar lines, Boeddeker and Hemmi (2010) have observed that bees in a rotating drum swayed and rolled their body around 0 deg while keeping their head in a stable orientation of either 0 deg or ±35 deg, which suggests the possible existence of different head and thorax control laws. For example, the model developed by Viollet and Zeil (2013) to account for head stabilization in wasps involves two different control pathways for the body and head, which are linked by an internal feedforward

Journal of Experimental Biology (2015) 218, 3777-3787 doi:10.1242/jeb.127043

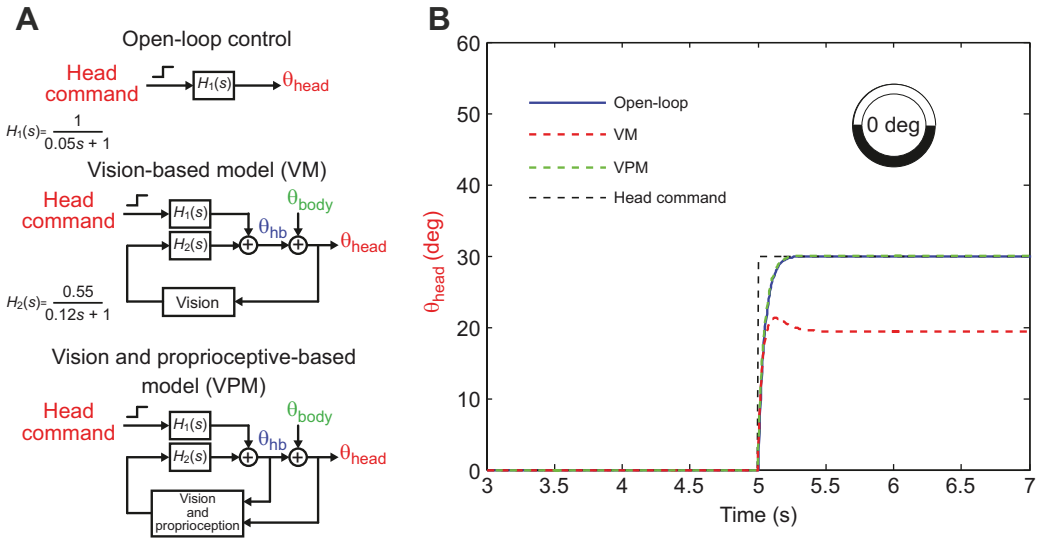

Fig. 10. Comparison of VM and VPM with regard to arbitrary head command. (A) Block diagram of three systems corresponding to an arbitrary head command (open loop) alone or combined with either a simple visual feedback reflex loop (VM) or a multisensory loop based on vision and neck proprioception organs (VPM) in response to a horizon. Dynamics of the response between arbitrary command [$H_1(s)$] and head locking to horizon reflex [$H_2(s)$] have been segregated to represent different control channels. We choose to represent the arbitrary command with a first-order transfer function, with a gain of 1 and a time constant of 0.05 s around that observed for head locking to horizon. (B) Simulations of the three model configuration to the induction of an arbitrary head command with a 0 deg horizon. Arbitrary command with a 30 deg amplitude step. The presence of a pure visual feedback loop based on horizon orientation interferes with a head command from another channel, whereas the feedback loop based on the estimation of body in horizon estimation allows complete response of any other head command channel.

control system. In addition, Hensler and Robert (1990) have reported that different body and head control processes are at work in locusts and discussed the possibility that non-linear proprioceptive inputs may be involved in the coordination between head and body roll control. The latter authors suggested that the observed linear relationship between head and body may be due to weaknesses of the experimental procedures used, and that in nature, flying insects must use coupled or uncoupled head/body control processes depending on the task (feeding, chasing, avoiding predation) they are performing. Likewise, in dragonflies, despite the differences between the head, which serves to track prey, and the body, which serves to intercept the trajectory of prey, prey-capture flight must be efficiently guided thanks to the integration of the signals generated by 'head in body' measurements (Olberg et al., 2007; Olberg, 2012; Mischiati et al., 2015). These studies suggest that the neck proprioceptor organs may serve as a gateway between two reference frames: the visual frame associated with the head, which serves as a reference frame during visually guided behaviour (Boeddeker and Hemmi, 2010) and the body frame associated with the thorax, on which locomotion is based. In addition to the idea that the head orientation may serve as a zero reference for controlling body roll movements (which are therefore based on 'head in body' inputs only), as proposed by Boeddeker and Hemmi (2010), the existence of an internal 'body in horizon' estimation suggested by our improved model would mean that the body control process based on the 'head in body' is liable to compensate for some visual errors by taking a reference body orientation with respect to the horizon. Body control in insects may therefore be enhanced by using the relative positions of the visual system, as established theoretically (Manecy et al., 2014) and this may account for the near-perfect hovering performances observed in some flying insects, including the hoverfly. In addition, a command based on an internal body roll estimation with respect to the horizon would give an arbitrary head command without any conflict with the two-nested feedback loop of the VPM (see Fig. 10). This configuration would therefore obviously have the advantage of making both the VPM and any other head control loop fully compatible. In other words, head control could be achieved by multiple channels without any need for identifying and switching between channels. It is of great importance to note that visually controlled stabilization of the head and body based on the orientation of the horizon does not require any gravity sense, which has never been observed in flies during flight so far (Hengstenberg, 1984). This hypothesis will now have to be tested experimentally using free roll procedures to study the head/body coordination triggered in response to body roll disturbances and dynamic rotations of the horizon.

One quite unexpected result obtained in this study focuses on the sex-related differences observed in the insects' head roll responses: the males feature slower but smaller steady-state errors in response to tilted horizons, but showed less head stability (see Fig. 3B). The main sex-related differences observed in hoverflies so far is the presence in the male compound eye of enlarged facets between the clypeus and ocellar triangle, which are absent in females (Collett and Land, 1975). This anatomical difference is associated with neural processing differences and the presence of a more accurate receptive field in males (Nordström et al., 2008) although female STMD neurons respond to the presence of small objects in the frontal visual field (Nordström and O'Carroll, 2006). The differences in head roll stabilization still remain to be explained, but they may be linked to behavioural differences such as mate chasing in males, which certainly requires specific stabilization abilities.

In conclusion, we have brought to light the existence in hoverflies of a horizon realignment reflex, which cannot be accounted for by a purely visual feedback under certain conditions. The improved model therefore developed to account for this behaviour was based on a multisensory integration pathway controlling the insects' head roll movements. On the basis of the responses obtained with this

model, we have put forward a new hypothesis on the combination of visual and proprioceptive information involved and the possibility that hoverflies may control their body roll orientation with respect to the horizon via proprioceptive sensors located in the neck joint.

Acknowledgements
We are greatly thankful to Julien Diperi for his work building the experimental device, to Marc Boyron developing the software and electronics on which all the work presented in this paper was based and to Jessica Blanc for correcting and improving the English manuscript. We are grateful to the reviewers for their useful comments.

Competing interests
The authors declare no competing or financial interests.

Author contributions
A.J.-L., J.F. and S.V. have designed the experiments. A.J.-L. and J.F. conceived the data analysis tools (tracking software). R.G. and S.V. conducted the experiments and interpreted the data. R.G., S.V., J.F. and J.-L.V. wrote the manuscript.

Funding
S.V. acknowledges support from the Centre National de la Recherche Scientifique (CNRS), Aix-Marseille University, the Agence Nationale de la Recherche (ANR) [with the EVA project (Autonomous Flying Entomopter) and the IRIS project (Intelligent Retina for Innovative Sensing) ANR-12-INSE-0009].

References
Berry, R., van Kleef, J. and Stange, G. (2007). The mapping of visual space by dragonfly lateral ocelli. *J. Comp. Physiol. A* **193**, 495-513.
Boeddeker, N. and Hemmi, J. M. (2010). Visual gaze control during peering flight manoeuvres in honeybees. *Proc. Biol. Sci.* **277**, 1209-1217.
Boeddeker, N., Dittmar, L., Stürzl, W. and Egelhaaf, M. (2010). The fine structure of honeybee head and body yaw movements in a homing task. *Proc. Biol. Sci.* **277**, 1899-1906.
Collett, T. S. and Land, M. F. (1975). Visual control of flight behaviour in the hover fly, Syritta pipiens L. *J. Comp. Physiol. A* **99**, 1-66.
Franklin, G. F., Powell, J. D. and Emami-Naeini, A. (1994). *Feedback Control of Dynamic Systems*. Reading, MA: Addison-Wesley.
Geiger, G. and Poggio, T. (1977). On head and body movements of flying flies. *Biol. Cybern.* **25**, 177-180.
Goodman, L. J. (1965). The role of certain optomotor reactions in regulating stability in the rolling plane during flight in the desert locust, *Schistocerca Gregaria*. *J. Exp. Biol.* **42**, 385-407.
Hedrick, T. L. (2008). Software techniques for two- and three-dimensional kinematic measurements of biological and biomimetic systems. *Bioinspir. Biomim.* **3**, 034001.
Hengstenberg, R. (1984). Roll-stabilization during flight of the Blowfly's head and body by mechanical and visual cues. In *Localization and Orientation in Biology and Engineering* (ed. D. Varju and H.-U. Schnitzler), pp. 121-133. Proceedings in Life Science. Springer-Verlag Berlin Heidelberg.
Hengstenberg, R. (1993). Multisensory control in insect oculomotor systems. In *Visual Motion and its Role in the Stabilization of Gaze* (ed. F. A. Miles and J. Wallman), pp. 285-298. Elsevier Science.
Hengstenberg, R. (1998). Controlling the fly's gyroscopes. *Nature* **392**, 757-758.
Hengstenberg, R., Sandeman, D. C. and Hengstenberg, B. (1986). Compensatory head roll in the blowfly *Calliphora* during flight. *Proc. Biol. Sci.* **227**, 455-482.
Hensler, K. and Robert, D. (1990). Compensatory head rolling during corrective flight steering in locusts. *J. Comp. Physiol. A* **166**, 685-693.
Horn, E. and Knapp, A. (1984). On the invariance of visual stimulus efficacy with respect to variable spatial positions. *J. Comp. Physiol. A* **154**, 555-567.
Horn, E. and Lang, H.-G. (1978). Positional head reflexes and the role of the prosternal organ in the walking fly, Calliphora erythrocephala. *J. Comp. Physiol. A* **126**, 137-146.
Hu, K. G., Reichert, H. and Stark, W. S. (1978). Electrophysiological characterization of *Drosophila* ocelli. *J. Comp. Physiol. A* **126**, 15-24.
Hung, Y.-S. and Ibbotson, M. R. (2014). Ocellar structure and neural innervation in the honeybee. *Front. Neuroanat.* **8**, 6.
Huston, S. J. and Krapp, H. G. (2009). Nonlinear integration of visual and haltere inputs in fly neck motor neurons. *J. Neurosci.* **29**, 13097-13105.
Land, M. F. (1973). Head movement of flies during visually guided flight. *Nature* **243**, 299-300.
Liske, E. (1977). The influence of head position on the flight behaviour of the fly. *Calliphora erythrocephala*. *J. Insect Physiol.* **23**, 375-379.
Manecy, A., Marchand, N. and Viollet, S. (2014). Hovering by gazing: a novel strategy for implementing saccadic flight-based navigation in GPS-denied environments. *Int. J. Adv. Robot. Syst.* **11**.
Milde, J. J., Seyan, H. S. and Strausfeld, N. J. (1987). The neck motor system of the fly *Calliphora erythrocephala*: II. Sensory organization. *J. Comp. Physiol. A* **160**, 225-238.
Mischiati, M., Lin, H.-T., Herold, P., Imler, E., Olberg, R. and Leonardo, A. (2015). Internal models direct dragonfly interception steering. *Nature* **517**, 333-338.
Mittelstaedt, H. (1950). Physiólogie des Gleichgewichtssinnes bei Fliegenden *Libellen*. *Z. Vergl. Physiol.* **32**, 422-463.
Nalbach, G. (1993). The halteres of the blowfly *Calliphora*. *J. Comp. Physiol. A* **173**, 293-300.
Neumann, T. R. and Bülthoff, H. H. (2001). Insect inspired visual control of translatory flight. In *Advances in Artificial Life* (ed. J. Kelemen and P. Sosik), pp. 627-636. Springer-Verlag Berlin Heidelberg.
Nordström, K. and O'Carroll, D. C. (2006). Small object detection neurons in female hoverflies. *Proc. Biol. Sci.* **273**, 1211-1216.
Nordström, K., Barnett, P. D., Moyer de Miguel, I. M., Brinkworth, R. S. A. and O'Carroll, D. C. (2008). Sexual dimorphism in the hoverfly motion vision pathway. *Curr. Biol.* **18**, 661-667.
Olberg, R. M. (1981). Parallel encoding of direction of wind, head, abdomen, and visual pattern movement by single interneurons in the dragonfly. *J. Comp. Physiol. A* **142**, 27-41.
Olberg, R. M. (2012). Visual control of prey-capture flight in dragonflies. *Curr. Opin. Neurobiol.* **22**, 267-271.
Olberg, R. M., Seaman, R. C., Coats, M. I. and Henry, A. F. (2007). Eye movements and target fixation during dragonfly prey-interception flights. *J. Comp. Physiol. A* **193**, 685-693.
Parsons, M. M., Krapp, H. G. and Laughlin, S. B. (2006). A motion-sensitive neurone responds to signals from the two visual systems of the blowfly, the compound eyes and ocelli. *J. Exp. Biol.* **209**, 4464-4474.
Paulk, A. and Gilbert, C. (2006). Proprioceptive encoding of head position in the black soldier fly, *Hermetia illucens* (L.) (Stratiomyidae). *J. Exp. Biol.* **209**, 3913-3924.
Peters, W. (1962). Die propriorezeptiven organe am prosternum und an den labellen von *Calliphora erythrocephala* mg. *Z. Morph. Ökol. Tiere* **51**, 211-226.
Preuss, T. and Hengstenberg, R. (1992). Structure and kinematics of the prosternal organs and their influence on head position in the blowfly *Calliphora erythrocephala* Meig. *J. Comp. Physiol. A* **171**, 483-493.
Pringle, J. W. S. (1938). Proprioception in Insects: III. The function of the hair sensilla at the joints. *J. Exp. Biol.* **15**, 467-473.
Schilstra, C. and van Hateren, J. H. (1998). Stabilizing gaze in flying blowflies. *Nature* **395**, 654.
Schuppe, H. and Hengstenberg, R. (1993). Optical properties of the ocelli of *Calliphora erythrocephala* and their role in the dorsal light response. *J. Comp. Physiol. A* **173**, 143-149.
Schwyn, D. A., Heras, F. J. H., Bolliger, G., Parsons, M. M., Krapp, H. G. and Tanaka, R. J. (2011). Interplay between Feedback and Feedforward Control in Fly Gaze Stabilization. In: *18th IFAC World Congress*, pp. 9674-9679.
Simmons, P. J., Jian, S. and Rind, F. C. (1994). Characterisation of large second-order ocellar neurones of the blowfly *Calliphora erythrocephala*. *J. Exp. Biol.* **191**, 231-245.
Stange, G. (1981). The ocellar component of flight equilibrium control in dragonflies. *J. Comp. Physiol. A* **141**, 335-347.
Stange, G., Stowe, S., Chahl, J. and Massaro, A. (2002). Anisotropic imaging in the dragonfly median ocellus: a matched filter for horizon detection. *J. Comp. Physiol. A* **188**, 455-467.
Strausfeld, N. J. and Seyan, H. S. (1985). Convergence of visual, haltere, and prosternal inputs at neck motor neurons of *Calliphora erythrocephala*. *Cell Tissue Res.* **240**, 601-615.
Taylor, C. P. (1981a). Contribution of compound eyes and ocelli to steering of locusts in flight: I. behavioural analysis. *J. Exp. Biol.* **93**, 1-18.
Taylor, C. P. (1981b). Contribution of compound eyes and ocelli to steering of locusts in flight: II. timing changes in flight motor units. *J. Exp. Biol.* **93**, 19-31.
Taylor, G. K. and Krapp, H. G. (2007). Sensory systems and flight stability: what do insects measure and why? *Adv. Insect Physiol.* **34**, 231-316.
Viollet, S. and Zeil, J. (2013). Feed-forward and visual feedback control of head roll orientation in wasps (*Polistes humilis*, Vespidae, Hymenoptera). *J. Exp. Biol.* **216**, 1280-1291.
Zar, J. H. (1996). *Biostatistical Analysis*, 3rd edn. Upper Saddle River:Prentice-Hall International, Inc.
Zeil, J., Boeddeker, N. and Hemmi, J. M. (2008). Vision and the organization of behaviour. *Curr. Biol.* **18**, R320-R323.